# Parallel-hat tempering: A Monte Carlo search scheme for the identification of low-energy structures

Yang Zhang and Jeffrey Skolnick[a)]
*Laboratory of Computational Genomics, Donald Danforth Plant Science Center, 893 North Warson Road, St. Louis, Missouri 63141*

(Received 10 May 2001; accepted 29 June 2001)

A new parallel-hat tempering algorithm has been developed for Monte Carlo simulations, in which a composite ensemble of noninteracting replicas of the molecule system at different temperatures is simulated, and the Markov process of each replica is driven by a hatlike weight factor with exponentially enhanced probability in both low- and high-energy regions. To test the algorithm, the methodology is applied to a homopolymeric protein chain located on a face-centered cubic lattice. We demonstrate that the ability of the current approach to search for low-energy molecule structures is significantly better than other Monte Carlo techniques found in the literature. © *2001 American Institute of Physics.* [DOI: 10.1063/1.1396672]

## I. INTRODUCTION

Predicting the three-dimensional structure of a protein from its amino acid sequence is a very important unsolved problem in biology. According to the *thermodynamic hypothesis* of Anfinsen,[1] the native structure of a protein corresponds to a global minimum of its free energy. However, since the energy landscape of the protein is characterized by numerous local minima separated by energy barriers, developing a powerful optimization method to search the minimum energy structure of a given protein potential remains a difficult, unsolved problem, despite the many efforts to solve it (see, e.g., Refs. 2–5).

A random search for the global minimum structure of a real protein is highly infeasible due to the extremely large number of possible conformations.[6] The most often used numerical technique found in the literature is to exploit the Monte Carlo simulation of equilibrium statistical mechanics, in which the protein starts from a randomly produced structure in a computer. Then its conformation is gradually modified according to a Metropolis selection criterion,[7] which favors the acceptance of the movement to the conformations of lower energies. To alleviate the problem of quasi-ergodicity arising from the roughness of the potential energy landscape, a variety of important improvements have been made (see, e.g., Refs. 8–16). In principle, the techniques utilized in these new approaches can be classified as one of two types. In the first, the Boltzmann weight is modified so that the simulation can be performed as a random walk in a desired energy-phase space. The new weight factor can be numerically attained by an iterative procedure; unfortunately, the rate of convergence is usually very slow for glassy systems, such as proteins below their glassy-transition temperature. A prominent example of this type of approach is the so-called entropy sampling Monte Carlo,[14] which is also known by a number of other names.[8,11,15] The second kind of approach is to implement the numerical simulation at different temperatures. Since, at high temperatures, the acceptance probability of a trial movement over a given energy barrier can be large, ergodicity can be implemented with reasonable ease in a Metropolis simulation. By exchanging states at different temperatures, the higher-temperature simulations can thus help the lower-temperature ones cross the energy barriers between different basins and thereby achieve ergodicity. This idea can be implemented either in a single simulation with a dynamic temperature (called simulated tempering[12,13]) or in several parallel simulations, each at a fixed temperature (called replica/parallel tempering[10,16]).

In previous work,[17] we applied both the entropy sampling and Monte Carlo replica exchange methods to study the collapse transition of a simple face-centered cubic (fcc) homopolymeric lattice polypeptide. It was found that, although both methods provide a complete thermodynamic description of the collapse transition, both entropy sampling Monte Carlo and classic Metropolis Monte Carlo are much more CPU time-consuming. However, the replica tempering method can more efficiently find low-energy conformations. It takes about one-tenth of the CPU time of the entropy method; furthermore, the average minimum energy obtained by the replica exchange method is about $5.7k_BT$ lower.[17]

Here we extend the replica method by the introduction of a new hatlike weight factor to each replica, in which both low- and high-energy acceptance probabilities are exponentially reinforced and the wider energy range can be explored in each simulation of a single replica. For comparison, we apply the proposed method to the same fcc protein model as done previously.[17] It is found that, within about the same CPU time as taken by the traditional replica exchange method, the search efficiency for minimum energy structures can be significantly increased by parallel-hat sampling.

[a)]Author to whom correspondence should be addressed.

 

## II. METHODS

### A. Weight factor

The weight factor utilized in this study is based on a previous weight function that has been successfully applied to explore equilibrium conformations of supercoiled DNA loops,[18] i.e.,

$$w(E)=\exp(-E/k_BT+\sqrt{2}|E-\langle E\rangle|/\sigma), \tag{1}$$

where $k_B$ is Boltzmann's constant, $\langle E\rangle$ is the average energy of the system at the temperature $T$, $\sigma\,(\sim k_BT)$ the root mean square deviation of the energy. Rather than deal with them as unknown parameters,[18] here we determine the values of $\langle E\rangle$ and $\sigma$ according to previously finished runs. At the $m$th step of the Monte Carlo process,

$$\begin{cases} \langle E\rangle=\dfrac{\sum_{i=1}^{m-1}E_i e^{-\sqrt{2}|E_i-\langle E\rangle_i|/\sigma_i}}{\sum_{i=1}^{m-1}e^{-\sqrt{2}|E_i-\langle E\rangle_i|/\sigma_i}}, \\ \sigma=\left[\dfrac{\sum_{i=1}^{m-1}E_i^2 e^{-\sqrt{2}|E_i-\langle E\rangle_i|/\sigma_i}}{\sum_{i=1}^{m-1}e^{-\sqrt{2}|E_i-\langle E\rangle_i|/\sigma_i}}-\left(\dfrac{\sum_{i=1}^{m-1}E_i e^{-\sqrt{2}|E_i-\langle E\rangle_i|/\sigma_i}}{\sum_{i=1}^{m-1}e^{-\sqrt{2}|E_i-\langle E\rangle_i|/\sigma_i}}\right)^2\right]^{1/2} \end{cases}, \tag{2}$$

where $\langle E\rangle_i$ and $\sigma_i$ denote, respectively, the average energy and standard deviation of the energy at the $i$th *step* of the simulation. Since the initial choices of the values of $\langle E\rangle$ and $\sigma$ do not significantly influence the final results, one can simply choose $\langle E\rangle=E$ in the initial few steps and then let the Boltzmann weight factor drive the simulation to the equilibrium states. Thus the new weight factor of Eq. (1) is known *a priori*, without free parameters that need to be determined before the Monte Carlo runs.

Figures 1(a) and 1(b) show the comparison of the time series of Monte Carlo simulations of an fcc polypeptide at $T=2\varepsilon_0/k_B$ (here, $\varepsilon_0$ is the unit of interaction energy. For the model description, see below or Ref. 17); these are calculated according to the canonical Boltzmann weight factor and the weight factor of Eq. (1), respectively. Since the simulations are implemented at a temperature $T$ higher than the critical point of the glassy transition of the system ($\sim 1.8\varepsilon_0/k_B$, see Ref. 17), both processes are not trapped in local energy basins. However, since in Eq. (1) both the low- and high-energy probabilities are reinforced, the sampling with the new weight factor explores a much wider energy range at the given temperature.

In Figs. 1(c) and 1(d), we show the distribution of energies sampled by these two weight factors (solid circles). While the sharp peak around the average energy of the canonical ensemble is exponentially damped by using the weight factor of Eq. (1), the new sampling in Fig. 1(d) has a wider hatlike spectral density. Since in the new sampling ensemble each conformation of energy $E_i$, in fact, represents a number of states $n_i(E_i)(=\exp[-\sqrt{2}|E_i-\langle E\rangle_i|/\sigma_i])$ in the real system, the physical expectation of any considered quantity $A$ should be calculated by

$$\langle A\rangle=\frac{\sum_{i=1}^{N_{\text{sweep}}}A(E_i)e^{-\sqrt{2}|E_i-\langle E\rangle_i|/\sigma_i}}{\sum_{i=1}^{N_{\text{sweep}}}e^{-\sqrt{2}|E_i-\langle E\rangle_i|/\sigma_i}}, \tag{3}$$

where $N_{\text{sweep}}$ is the number of sweeps of the Monte Carlo sampling. As an illustration, we show in Fig. 1(d) (squared symbols) the canonical energy distribution reweighted from the hatlike sampling through Eq. (3). As expected, the rescaled energy distribution is the same as that calculated by the canonical Metropolis sampling at high temperature [Fig. 1(c)].

The physical origin of the enhanced efficiency of this hatlike sampling method can be understood as follows: According to Eq. (1), a Monte Carlo movement from conformation 1 to conformation 2 over an energy barrier of $\Delta E=E_2-E_1$ is accepted with a probability,

$$\begin{aligned} p_{1\to 2}&=\exp(-\tilde{\beta}\Delta E) \\ &=\exp[-\beta\Delta E+\sqrt{2}/\sigma(|E_2-\langle E\rangle|-|E_1-\langle E\rangle|)], \end{aligned} \tag{4}$$

where $\beta\equiv 1/k_BT$ is the general inverse temperature. The hatlike sampling process with fixed temperature can therefore be interpreted as a Monte Carlo process with an energy dependent dynamic temperature. At lower energy values $[(E<\langle E\rangle),\ \tilde{\beta}=\beta+\sqrt{2}/\sigma]$ the simulation is implemented at an effectively lower temperature, which enables the simulation to scan, in a more detailed manner, the lower-energy structures at low-energy basins of the landscape, as indicated in Fig. 1(b). In the higher-energy region $[(E>\langle E\rangle),\ \tilde{\beta}=\beta-\sqrt{2}/\sigma]$ where the effective temperature rises, keeping the simulation from being trapped for too long of a time in one low-energy basin, the Monte Carlo process is able to more extensively explore additional energy regions. The dynamic temperature is thus automatically optimized as the simulation proceeds.

### B. Parallel-hat sampling

The idea of parallel sampling here is similar to those previously used,[10,12,13,16] in which artificial ensembles consisting of $M$ noninteracting replicas of the investigated molecule system are considered, each at a distinct and fixed temperature. The basic object of the numerical simulation is to

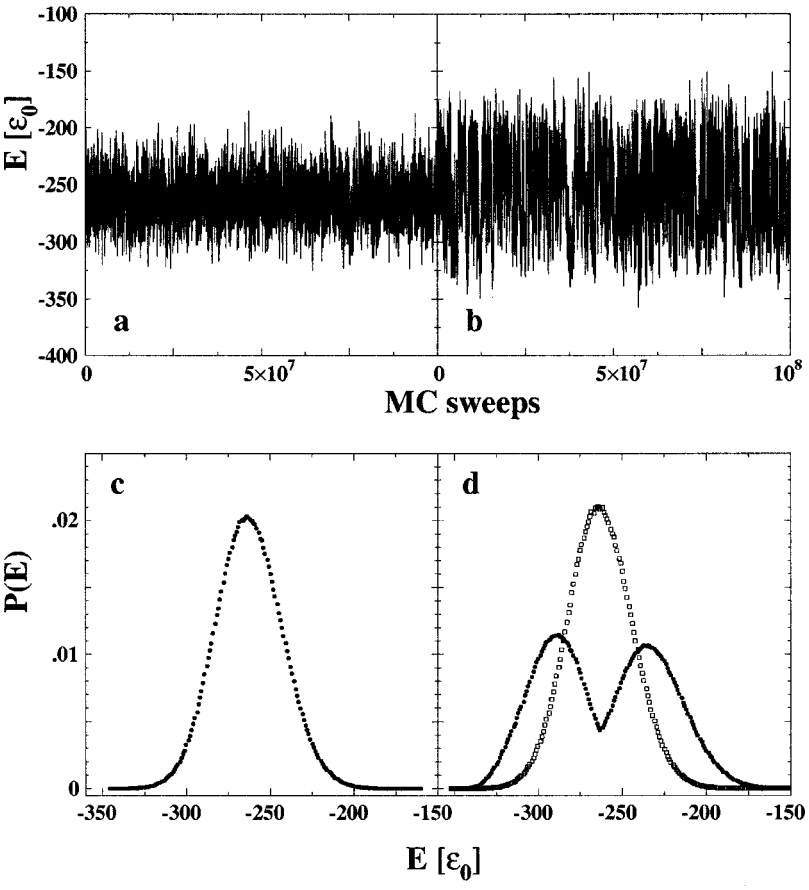


FIG. 1. Comparison of two Monte Carlo implementations of single replicas at temperature $T=2\varepsilon_0/k_B$, driven by the canonical Boltzmann weight factor and the factor of Eq. (1), respectively. (a) The time series of system energy driven by the Boltzmann factor (one point for every 10 000 Monte Carlo updates is shown here); (b) the time series of the energy driven by Eq. (1); (c) an energy histogram sampled with the Boltzmann factor; (d) an energy histogram (solid circles) sampled by Eq. (1), the squared symbols denote the energy distribution rescaled from the hat sampling by Eq. (3).

construct a Markov-chain that will ensure that the corresponding thermodynamic equilibrium will be approached for the composite artificial ensemble.

To guarantee that the ergodicity and detailed balance conditions hold, the following two sets of movements are taken into account in our simulations:

(i) Local movements in each replica. Each trial movement is accepted or rejected according to Eq. (4).

(ii) Swap movements of global conformations between two replicas (say, $i$ and $j$). The acceptance probability of each swap is

$$p_{i\leftrightarrow j}=\alpha\exp[(\beta_i-\beta_j)(E_i-E_j)], \tag{5}$$

where

$$\ln\alpha=\sqrt{2}(|E_j-\langle E_i\rangle|/\sigma_i-|E_i-\langle E_i\rangle|/\sigma_i +|E_i-\langle E_j\rangle|/\sigma_j-|E_j-\langle E_j\rangle|/\sigma_j). \tag{6}$$

While it is not necessary to restrict the swap to pairs of replicas associated with neighboring inverse temperatures $\beta_i$ and $\beta_{i+1}$, this choice will be optimal since the acceptance ratio will decrease about exponentially with the difference $\Delta\beta=\beta_i-\beta_j$.

An important question which remains to be settled in parallel-hat sampling is how often should the swap moves be done. The basic motivations of the parallel method is to let higher-temperature simulations help the lower-temperature one across the energy barriers. The algorithm will clearly not be efficient if the swap facilitates the exchange before the higher-temperature simulation can jump out from its original energy basin. The general criterion for choosing the swapping frequency is to follow the energy of the *higher-temperature* simulation until it has passed through values significantly different from the initial value. This time scale can be quantitatively estimated by the integrated autocorrelation time $\tau$:

$$\tau=\int_0^\infty\frac{\chi(t)}{\chi(0)}dt, \tag{7}$$

where the time-displaced autocorrelation function $\chi(t)$ of the system energy is defined as

$$\chi(t)=\int_0^{t_{\max}-t}dt'[(E(t')-\langle E\rangle)(E(t'+t)-\langle E\rangle)], \tag{8}$$

and $t_{\max}$ is the maximum number of Monte Carlo steps in the single replica simulation.

In Fig. 2, we show the values $\tau$ as a function of temperature $T$ for the fcc polypeptide using parallel-hat sampling. The autocorrelation time of Monte Carlo processes below the glassy transition is about ten-fold larger than that above the glassy transition. This correlation characteristic of glassy-transition systems is dramatically different from that of a normal transition. In a normal transition system, e.g., a two-dimensional spin system[19] or single-stranded DNA polymers,[20] the autocorrelation time $\tau$ singularly diverges at the phase transition temperature (well-known as the *critical*

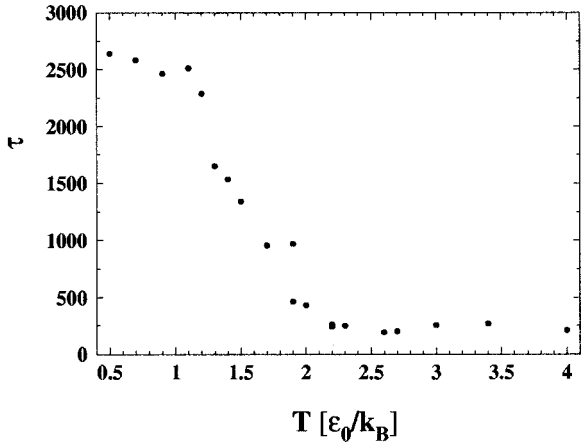


FIG. 2. The autocorrelation time $\tau$ of the energy as a function of replica temperature. The values of $\tau$ are scaled by the chain length, $N=64$. Data are obtained from $2\times10^8$ Monte Carlo iterations of parallel-hat sampling of 19 replicas. The statistical error bars are inside the symbols.

*slowing down* effect), and the value of $\tau$ is at the same order of magnitude when below and above the transition temperature.[20]

Around the transition point, the correlation time of the present simulation falls off roughly exponentially from lower to higher temperature (Fig. 2). This exponential fall-off in correlation time is important for the rapid equilibration of the algorithm. Below the glassy-transition point, the correlation time $\tau$ does not obviously increase with decreasing temperature, which signifies that the parallel-hat tempering method does work at overcoming the problem of quasi-ergodicity for the simulation at low temperature.

Keeping in mind the data in Fig. 2, the optimal choice of swap frequency in our simulation would be to make *one* global conformation swap of each neighboring replica pair realized in approximately *each* $\tau$ *steps*, where $\tau$ is of course determined from the higher-temperature replica of the swapping replica pair.

## III. RESULTS AND DISCUSSION

Throughout this paper, we apply the proposed algorithm to homopolymeric chains located on a face-centered cubic (fcc) lattice system. The fcc lattice system can be defined as a set of points $(i,j,k)$ on a normal three-dimensional lattice system where the sum of $i+j+k$ is even. Each node in the fcc system has 12 neighbors, which makes the polymer chains on the fcc lattice system assume the relatively larger number of conformations and effects of residue connectivity and packing than that in the normal lattice system (each node with six neighbors). This lattice structure is also the most typical lattice structure for the majority of crystalline metals.[21]

Our polymer is a self-avoiding chain consisting of $N$ united residues (or atoms) with a fixed bond length of $\sqrt{2}$, which equals the distance between neighboring fcc nodes. The residues are located on the nodes of the fcc lattice. The polymer assumes a variety of conformations depending on the bond angle of each vertex that is allowed to be 60, 90, 120, or 180 degrees.

To mimic the proteinlike local conformational preference of $\beta$-type structures and the average hydrophobic attraction between chain units, two elemental force fields are assumed to be operative in the chain: one for long-range and one for short-range interactions. The long-range interactions are assumed to work in such a way that the energy of the system decreases by $\varepsilon_A$ when one of the nonadjacent residue pairs occupies the nearest-neighbor lattice points, i.e., their distance is $\sqrt{2}$. The short-range force is associated with the relative angles of three neighboring bonds. The system's energy will be decreased by $\varepsilon_B$ when their consecutive bonds are in an expanded conformation, i.e., when it satisfies the following conditions: (1) the angle of the first and second bonds and the angle of second and third bonds are both larger than 90 degrees, and (2) the angle of first and third bonds (oriented along the chain) is less than 90 degrees.

For convenience of comparison to previous work,[17] which examined the abilities of various Monte Carlo algorithms to find lowest-energy structures, here we have also used the same model parameters in our calculations, i.e., chain length $N=64$ and force field strength $\varepsilon_B=4\varepsilon_A=4\varepsilon_0$, where $\varepsilon_0$ is the scale of interaction energy serving to define the dimensionless temperature $T$ (in units of $\varepsilon_0/k_B$ as mentioned above). Two types of similar local movements as in Ref. 17 are considered in our simulations. The first involves a random rotation of a randomly chosen two-bond subchain; the second involves random rotations of the chain ends around the last second residue. Both movements should guarantee that the rotated residues are on the fcc lattices and that the bond lengths remain unchanged.

In order to optimize the implementation of the replica-hat method, an appropriate temperature set should be chosen. Generally, the lowest temperature should be the one at which a single simulation could get trapped in a local energy basin; the highest temperature has to be chosen such that any energy barrier can be crossed with reasonable ease in a single simulation. To guarantee appropriate communication between neighboring samples, the temperature separations

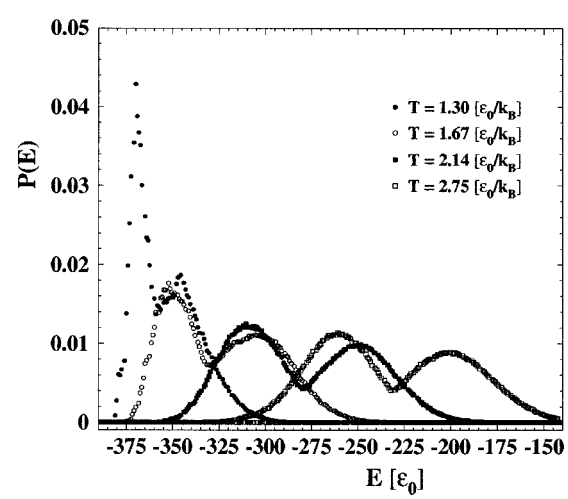


FIG. 3. The energy distribution of different replicas in a representative running of parallel-hat sampling. A total of $2\times10^8$ Monte Carlo steps are performed in the simulation, in which $5\times10^7$ iterations are performed for each replica.

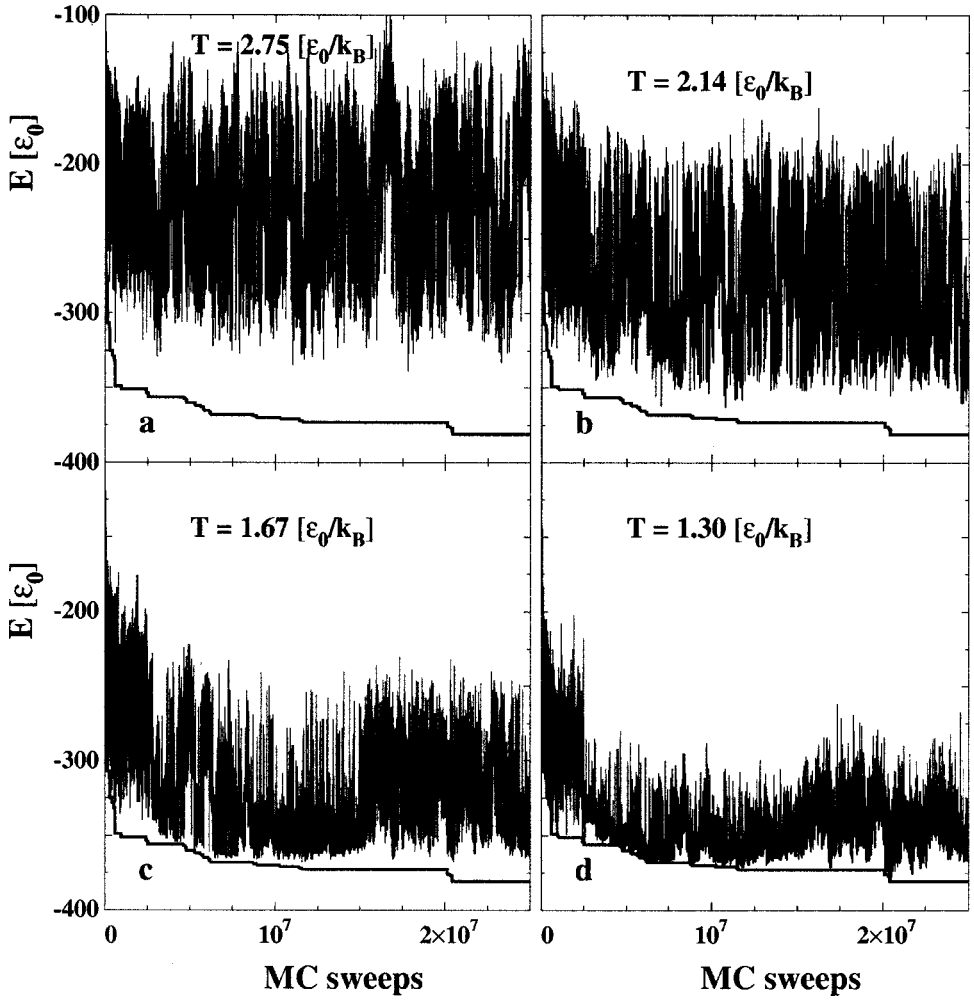


FIG. 4. Energies of individual replicas as function of Monte Carlo steps in parallel-hat simulation. One point is drawn for every 200 sweeps. Here, only the first $10^8$ Monte Carlo steps are shown out of the $2\times10^8$ runs. The thick line denotes the current lowest energy found in the sampling.

should be chosen so that the energy density of neighboring replicas have a small overlap region. Since the single-hat sampling has a wider energy spectrum than Metropolis sampling for a given temperature, fewer replicas are needed in parallel-hat sampling to cover the desired energy space than in normal replica sampling.

As a representative example, we show in Fig. 3 the energy distribution of different temperatures, obtained from a parallel-hat tempering simulation with four replicas and $5\times10^7$ Monte Carlo iterations for each replica. In this simulation, a temperature set of exponentially changed temperature increments was chosen and the frequency of swap movements in each neighboring replica pairs was adjusted to approximately match the autocorrelation time of the higher-temperature replica according to the data in Fig. 2.

The time series of the energy found in the four replicas are displayed in Fig. 4. It is shown that the minimum energy structures of the molecule system are mainly explored by the lowest-temperature replica, and the highest-temperature process serves to transform the composite ensemble from one region of energy-phase space to another. The replicas of intermediate temperatures serve to facilitate communication between these two replicas.

In Table I, we divide the whole Monte Carlo run (of $2\times10^8$ iterations) into 20 subsamples and record the minimum energy $E_{\min}$ of the molecule system in each subsample. For a comparison, we also show the result of a regular replica run using the temperature parameters which have been optimized in Ref. 17. According to Table I, the replica-hat sampling explores lower-energy structures than replica exchange in most subsamples. The average minimum energy in the 20 subsamples is about $5\,k_BT$ lower than that found by regular replica sampling. The difference of the lowest observed energies in these two representative runs is more than $10\,k_BT$ (see Table I). The structures of lowest energies explored by the two algorithms are displayed in Fig. 5. Although it is not sure at this moment whether the structure of $E=-387\varepsilon_0$ is the native structure of the global minimum in the considered model system, the lower-energy conformation is more compact and symmetrical than that found by replica exchange Monte Carlo alone (Fig. 5).

To further examine the abilities of these two methods to search low-energy structures, we performed ten independent Monte Carlo runs for both algorithms, each with different starting structures and random number seeds. The average result for lowest-energy states are summarized in Table II. The table also provides a comparison of the cost of computation on a 750 MHz Pentium III processor. In a similar amount of CPU time, the average minimum energy found by

TABLE I. Comparison of two representative Monte Carlo runs (of $2\times10^8$ iterations) by the parallel-hat sampling and regular replica sampling methods, respectively. The whole samples are divided into 20 subsamples. The shows are the lowest energies $E_{\min}$ (in unit of $\varepsilon_0$) explored in sequential subsamples, each including $10^7$ iterations.

| Order of subsample | Parallel-hat sampling | Replica sampling |
|---|---|---|
| 1 | −354 | −354 |
| 2 | −360 | −363 |
| 3 | −368 | −367 |
| 4 | −370 | −367 |
| 5 | −373 | −357 |
| 6 | −370 | −363 |
| 7 | −371 | −364 |
| 8 | −368 | −368 |
| 9 | −381 | −367 |
| 10 | −368 | −370 |
| 11 | −383 | −368 |
| 12 | −370 | −368 |
| 13 | −369 | −366 |
| 14 | −378 | −368 |
| 15 | −371 | −372 |
| 16 | −387 | −371 |
| 17 | −371 | −369 |
| 18 | −383 | −375 |
| 19 | −370 | −372 |
| 20 | −377 | −372 |
| $\langle E_{\min}\rangle$ | $-372.10\pm1.74$ | $-367.05\pm1.13$ |
| Lowest $E_{\min}$ | −387 | −375 |

parallel-hat sampling is $8.8\,K_BT$ lower than that obtained by regular replica sampling, which is numerically even larger than the difference ($\sim5.7\,k_BT$) between the replica sampling and entropy sampling methods.[17] Bearing in mind that the lower the energy that is accessed, the more difficult the searching process becomes, this enhancement in search ability is of qualitative significance.

## IV. CONCLUSION

In this work, we extend the replica-tempering Monte Carlo algorithm by the introduction of a hatlike weight factor in each replica simulation. With this *a priori* known weight factor, the sampling probability of the low- and high-energy regions is exponentially enhanced, and a wider range of phase space can be explored by a single replica at a given fixed temperature than when the Boltzmann weight factor is used. We applied the new Monte Carlo algorithm to the numerical simulation of a simplified homopolymeric protein model confined to a fcc lattice. The results show that, for about the same CPU time, significantly lower-energy regions of the considered molecule system are explored by the parallel-hat sampling method than that by regular replica exchange MC. Combined with previous Monte Carlo implementations of different methods,[17] it is concluded that the ability of the present algorithm to search the minimum energy structure is greater than other Monte Carlo algorithms, including the regular Metropolis sampling, entropy sampling, and replica sampling.

Last but not least, the physical expectation of a desired quantity in our simulation can be calculated according to the reweighting formula of Eq. (3). From this, the complete thermodynamic description of the molecule system can be straightforwardly obtained by the present algorithm. Although this is not the focus of this work, our unpublished data have confirmed that similar results concerning the system's thermodynamics are obtained by parallel-hat sampling, as compared to the entropy sampling and replica sampling methods.

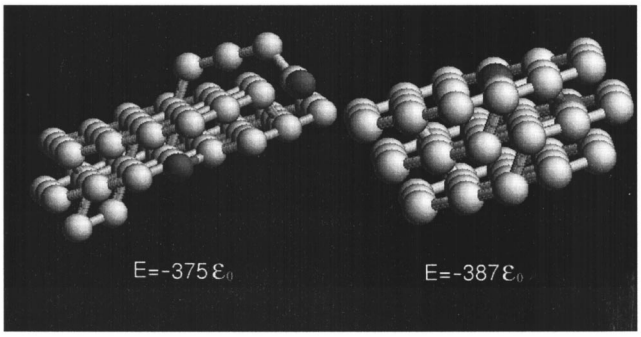


FIG. 5. The lowest-energy structures and the energies of the fcc homopolymeric chain as identified by regular replica sampling (left) and parallel-hat sampling (right) methods in a representative running of $2\times10^8$ Monte Carlo iterations. For the sake of clarity, the N and C termini are in dark gray.

TABLE II. Comparison of ten independent Monte Carlo runs for parallel-hat sampling (PHS) and regular replica sampling (RS), each of which starts with different initial structures and different seeds for the random number generator. The number of iterations in each run is $2\times10^8$ steps.

| | Number of replicas | Average CPU time | Average minimum energy ($\varepsilon_0$) |
|---|---|---|---|
| PHS | 4 | 4 h 32 min | $380.4\pm1.86$ |
| RS | 5 | 4 h 10 min | $371.6\pm1.28$ |

## ACKNOWLEDGMENT

This research was supported in part by NIH Grant No. GM-37408.

[1] C. B. Anfinsen, Science **181**, 223 (1973).
[2] J. Lee, H. A. Scheraga, and S. Rackovsky, J. Comput. Chem. **18**, 1222 (1997).
[3] P. Derreumaux, J. Chem. Phys. **106**, 5260 (1997).
[4] D. J. Wales and H. A. Scheraga, Science **285**, 1368 (1999).
[5] G. Stolovitzky and B. J. Berne, Proc. Natl. Acad. Sci. U.S.A. **97**, 11164 (2000).
[6] B. A. Reva, A. V. Finkelstein, and J. Skolnick, Folding Des. **3**, 141 (1998).
[7] N. Metropolis, A. W. Rosenbluth, M. N. Rosenbluth, and A. H. Teller, J. Chem. Phys. **21**, 1087 (1953).
[8] G. M. Torrie and J. P. Valleau, J. Comput. Chem. **23**, 187 (1977).
[9] S. Kirkpatrick, C. D. Gelatt, and M. P. Vecchi, Science **220**, 4598 (1983).
[10] R. H. Swendsen and J. S. Wang, Phys. Rev. Lett. **57**, 2607 (1986).
[11] B. A. Berg and T. Neuhaus, Phys. Rev. Lett. **68**, 9 (1992).
[12] A. P. Lyubartsev, A. A. Martsinovski, S. V. Shevkunov, and P. N. Voronstsov-Velyaminov, J. Chem. Phys. **96**, 1776 (1992).
[13] E. Marinari and G. Parisi, Europhys. Lett. **19**, 451 (1992).
[14] J. Lee, Phys. Rev. Lett. **71**, 211 (1993).
[15] U. H. E. Hansmann and Y. Okamoto, J. Comput. Chem. **14**, 1333 (1993).
[16] U. H. E. Hansmann, Chem. Phys. Lett. **281**, 140 (1997).
[17] D. Gront, A. Kolinski, and J. Skolnick, J. Chem. Phys. **113**, 5065 (2000).
[18] Y. Zhang, Phys. Rev. E **62**, R5923 (2000).
[19] M. E. J. Newman and G. T. Barkma, *Monte Carlo Methods in Statistical Physics* (Clarendon, Oxford, 1999).
[20] Y. Zhang, H. J. Zhou, and Z.-C. Ou-yang, Biophys. J. **81**, 1133 (2001).
[21] N. W. Ashcroft and N. D. Mermin, *Solid State Physics* (Saunders College Publishing, Orlando, 1976).